

INTERNATIONAL SOCIETY FOR SOIL MECHANICS AND GEOTECHNICAL ENGINEERING



This paper was downloaded from the Online Library of the International Society for Soil Mechanics and Geotechnical Engineering (ISSMGE). The library is available here:

<https://www.issmge.org/publications/online-library>

This is an open-access database that archives thousands of papers published under the Auspices of the ISSMGE and maintained by the Innovation and Development Committee of ISSMGE.

The paper was published in the proceedings of the 6th International Conference on Geotechnical and Geophysical Site Characterization and was edited by Tamás Huszák, András Mahler and Edina Koch. The conference was originally scheduled to be held in Budapest, Hungary in 2020, but due to the COVID-19 pandemic, it was held online from September 26th to September 29th 2021.

Spatial variability of relative density of sandy seabed surface sediments in an energetic nearshore zone estimated from a portable free fall penetrometer

Nina Stark

Virginia Tech, Blacksburg, USA, ninas@vt.edu

Nick Brill, Ali Albat, Reem Jaber, Dennis Kiptoo

Virginia Tech, Blacksburg, USA, nickb96@vt.edu, ali2@vt.edu, reemj@vt.edu, dkiptoo@vt.edu

ABSTRACT: Many nearshore environments are characterized by energetic hydrodynamic conditions and active sediment transport processes. This impacts coastal erosion and vulnerability, as well as engineering activities in the coastal zone. Friction angle and relative density are key parameters affecting sediment erodibility and soil behavior. However, they have rarely been quantified due to the increased complexity of extracting high quality samples of cohesionless sediments under energetic hydrodynamics. In this study, variations in relative density across and along the sandy nearshore zone of Phipps Peninsula in Yakutat, Alaska, were estimated using a portable free fall penetrometer. Preliminary results suggest significant variations in relative density ($D_r = \sim 20\text{-}95\%$) of sandy surface sediments along four cross-shore profiles (distance to shoreline approximately 200-550 m). These variations were associated with the expected wave impact on the seabed and local sediment transport processes, suggesting also a relationship to water depth and wave height.

Keywords: nearshore zone; sand; portable free fall penetrometer; relative density.

1. Introduction

The nearshore zone can be defined as the area stretching from the shoreline towards offshore to a water depth at which waves are not interacting with the seafloor anymore [1]. This bathymetric line or water depth is also often defined as the wave base where even during high swell events no sedimentary particles are mobilized by wave-induced water motion [2]. Thus, the nearshore zone is subjected to significant geomorphodynamics, possibly including the evolution and destruction of nearshore bars, with variations in wave conditions. Such processes can affect navigation and recreational beach users (e.g., in terms of rip currents and surf), as well as impact engineering activities and the interaction with infrastructure. Therefore, there is a need to fully understand nearshore geomorphodynamics under varying wave conditions and to predict the resulting nearshore and coastline evolution.

A large number of previous studies have documented nearshore geomorphodynamics in energetic wave condition, and predictive models have been developed [3-8]. Most of these studies include detailed information about local hydrodynamics and bathymetry. However, when considering the sediment properties, most studies and models focus on grain size distributions only, although the relevance of properties such as bulk density (i.e., particle packing and soil texture) as well as friction angles for sediment transport and reorganization processes has been acknowledged [9-11]. More specifically, Caballeria et al. (2002) highlight the importance of sand porosity for sediment self-organization processes in nearshore environments [11]. Sand porosity depends on particle shapes and size distribution, but also on the packing order and

density, and therefore, is directly related to relative density of the sand. Thus, relative density of sandy sediments has likely significant effects on local sediment remobilization in nearshore environments.

Albat et al. (2019) documented significant variations in surficial sediment strength and associated estimated friction angles in the energetic nearshore zone of Duck, North Carolina, USA [12]. These variations are likely affected by differences in sand bulk density or the relative density of the sand, as differences in grain size distributions and particle shapes were limited. Albat et al. (2020) propose a relationship between relative density of nearshore sand to its in-situ friction angle, and how this can be estimated from portable free fall penetrometer measurements [13].

This study represents a preliminary attempt to investigate variations of relative density of sandy nearshore sediments in an environment known for its energetic wave climate. The variations in relative density in the nearshore zone are discussed with regards to recent sediment remobilization processes. Field measurements were collected in the nearshore zone of the Phipps Peninsula including Cannon Beach, Ocean Cape and Point Carver in Yakutat, Alaska. The specific research objectives include (i) testing the applicability of a portable free fall penetrometer and the method proposed by Albat et al. (2020) [13] for estimating variations in in-situ relative density of nearshore sands, and (ii) the discussion of the results in the context of local sediment remobilization processes.

2. Regional context

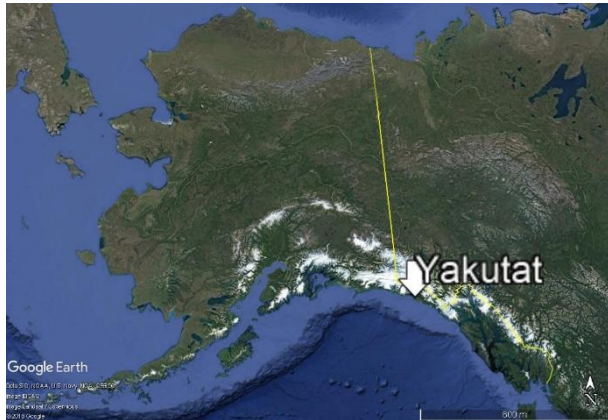


Figure 1. Google Earth (2019) image showing the location of Yakutat in the geographical context of Alaska and the northwest of Canada [31].

The City and Borough of Yakutat is located in southeast Alaska and is fringed by glaciers, mountains and the Gulf of Alaska (Fig. 1). Phipps Peninsula features Cannon Beach facing the Southwest, Ocean Cape facing Northwest and Point Carrew inside of Yakutat Bay (Fig. 2). Tschetter et al. (2016) documented most energetic waves approaching from the South and Southwest [14]. Thus, Cannon Beach is exposed to an energetic wave climate, while waves are refracting around Ocean Cape and Point Carrew in most conditions. This leads to often obliquely approaching waves at the latter two locations. Maximum significant wave heights of up to 10 m were measured [14]. Cannon Beach has been investigated for the development of wave energy harvesting.

Fine quartz sand with rock fragments with a mean particle size between 0.2-0.3 mm (poorly graded fine sand according to the Unified Soil Classification System-ASTM D2487) were documented by Ruby (1977) [15]. This author also highlighted finer sediments in the subaerial and higher intertidal zone and coarser sediments in the lower intertidal zone. Earlier Wright (1972) also stressed a significant abundance of heavy minerals such as titanium and gold in the beach sediments [16].

All three beaches can be considered wide (width > 100 m) with the wide sand spit at Point Carrew reaching a width in excess of 500 m. They also all exhibit a dynamic beach profile with a vegetated berm at Cannon Beach, a cobbly beach step at Ocean Cape (Fig. 2 and 3), and the occasional evolution and destruction of a ridge-runnel system at all three locations (Fig. 3). Ridge-runnel beach morphologies have been associated with a low relative tidal range (i.e., ratio between tidal range and breaker height) and medium to high dimensionless fall velocities (i.e., the ratio between breaker height and the particle fall velocity multiplied by the wave period) [17]. Thus, ridge runnel systems are representative of an energetic wave climate. Furthermore, ridge-runnel beach morphologies complicate cross-shore moisture content profiles and ground water behavior. The depressed runnel sustains water, while the crest of the runnel may drain better than the same sand at the same cross-shore location with a smoothly sloped beach morphology [18]. Albat and Stark (2016) documented the presence of a nearshore bar



Figure 2. Google Earth (2019) image showing Phipps Peninsula with Cannon Beach, Ocean Cape, and Point Carrew [31].



Figure 3. Photo of runnel at Ocean Cape in 2019. In the foreground, wet soil in the runnel and a sharp edge to the sand ridge can be seen. The shoreline of the Gulf of Alaska is visible in the background. Some cobbles were deposited in the runnel, and the portable free fall penetrometer is sitting after deployment in the runnel.

offshore of Cannon Beach [19]. However, no other bathymetric surveys in the area detected a bar [14]. This may suggest an occasional formation and destruction of nearshore bar systems. The complex and localized geomorphodynamics as well as complex groundwater and surface water interactions also lead to the hypothesis that spatial variations in surficial relative density of sandy sediments can be expected at the beach as well as in the nearshore zone through the frequent exchange of sediments between the beach and the nearshore zone. Figure 3 shows a wet and well developed runnel with a sharp edge transition to the ridge and the shoreline in the background. It also shows the deposition of cobbles in the runnel. The photo was taken in August 2019 at Ocean Cape. No ridge-runnel was observed at the same location and time of the year in 2018.

3. Methods

Portable free fall penetrometer (PFFP) deployments were carried out in 2018 and 2019 along cross-shore directed (perpendicular to the shoreline) and long-shore directed (parallel to the shoreline) transects in water depths ranging from approximately 3-30 m around



Figure 4. Photo of PFFP *BlueDrop* after deployment in muddy sediments.

Phipps Peninsula. In both years, PFFP deployments were also conducted in the intertidal zone, but those measurements are out of the scope of this article.

The PFFP used is the *BlueDrop* (Fig. 4) with a weight of approximately 7.5 kg and a length of ~64 cm. The PFFP was deployed manually (i.e., no support from a winch or capstan) from a small landing vessel (length of approximately 8 m) in the nearshore zone of the Phipps Peninsula. Bathymetric measurements of the same transects were performed using different acoustic hydrographic tools, but those measurements are out of the scope of this article. During deployment, the PFFP is released, free falls through the water columns, impacts and penetrates the seabed until the momentum is depleted. A principal difference between free fall penetrometers and conventional Cone Penetration Testing (CPT) is that free fall penetrometers are driven into the soil by their own weight and momentum, while CPT are often driven by external forces (e.g., hydraulic reaction frames). PFFP represent a particularly small and lightweight design of free fall penetrometers enabling deployment by hand in challenging areas and/or with limited resources. Here, energetic wave conditions challenge the use of larger vessels or more complex geotechnical instruments in the nearshore zone.

The PFFP *BlueDrop* measures vertical acceleration using five microelectromechanical systems (MEMS) accelerometers with different ranges and accuracies providing information about the probe's motion and the soil's resistance that is governing the probe's motion during penetration. The device also measures tilt using a dual-axis MEMS accelerometer. Deployments featuring significant inclination ($> 5\text{-}10^\circ$) of the probe from the vertical were discarded from analysis. Finally, the device records ambient pressure, including hydrostatic pressure in the water column and pore pressure during penetration, behind the cone (comparable to the CPT u_2 position).

In this study, the method to estimate in-situ relative density of nearshore sands by Albat (2018) was applied [20]. The author conducted controlled laboratory tests deploying the same PFFP at similar impact velocities as typical for field measurements into a sand sample prepared to relative densities of 23%, 45%, 70% and 80%. The sand was representative of grain size

distributions obtained from sampling at Cannon Beach (i.e., also of Ocean Cape), and the relative densities were achieved through a sand pluviation system. Based on these laboratory tests, the following correlation between the relative density of the sand, D_r , and the maximum deceleration measured by the PFFP, a [20] was obtained:

$$D_r = -14.66 \times 10^{-3} a^2 + 2.66a - 25.17 \quad (1)$$

Based on ten controlled laboratory tests, this correlation yielded $R^2=0.99$, representing an excellent match. It should be noted that Albat et al. (2019) explored this relationship further [13], but for this preliminary investigation, the original expression from Albat (2018) [20] was applied to four cross-shore transects in the nearshore zone of Phipps Peninsula with focus on Ocean Cape and Point Carrew (Fig. 5), and variations in relative density in those environments.

4. Results & Discussion

The measured transects are shown in Figure 5. In this article, results from transect K19 (with 8 deployment locations along the transect), transect L19 (with 8 deployment locations along the transect), transect A18 (with 12 deployment locations along the transect), and transect D18 (with 6 deployment locations along the transect) will be presented. The numbers in the transect nomenclature refer to the year of measurements.

Figure 6 shows the measured deceleration at way-point (WPT) #418 on transect A18. This location was approximately 430 m from the shoreline, representing one of the most offshore deployments along this transect. From ~ 4 cm of penetration depth towards the maximum deceleration an approximately steady increase in the probe's deceleration was measured, being indicative of a steadily increasing resistance of the seabed against the probe with penetration depth. Only in the uppermost 2-4 cm somewhat of a looser sediment layer can be interpreted. The penetration depth is limited to about 13 cm, reflecting merely seabed surface conditions. This is typical of this device in this type of sands [19]. The maximum deceleration is nevertheless only about 20 g with g being gravitational acceleration. This is a rather small value for sandy nearshore sediments [12, 13]. After reaching the maximum deceleration, the probe comes rapidly to a stop



Figure 5. Google Earth (2019) image with measured transect lines: cross-shore transects measured in 2018 in blue, cross-shore transects measured in 2019 in red, and longshore transects in magenta. Transects of relevance to this article are labeled [31].

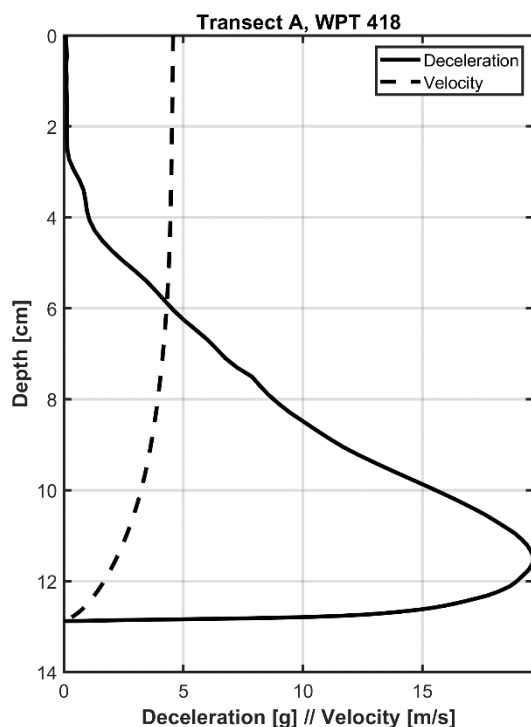


Figure 6. Penetration depth versus measured deceleration (solid line) and penetration velocity (dashed line) at waypoint #418 on transect A18, located about 430 m offshore of the shoreline.

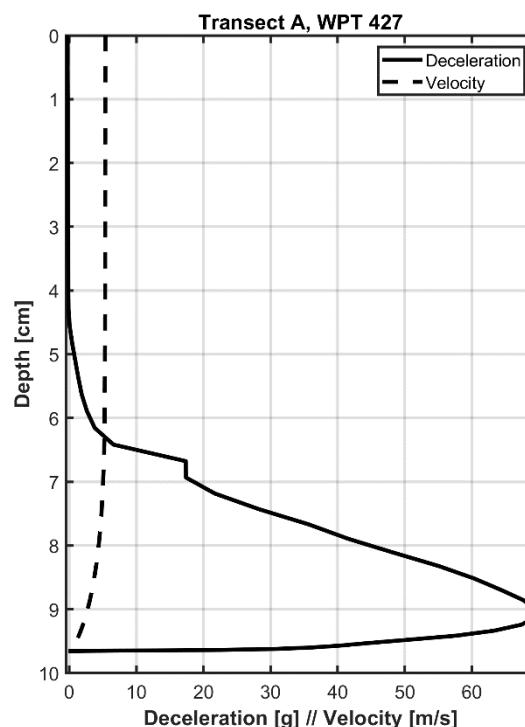


Figure 7. Penetration depth versus measured deceleration (solid line) and penetration velocity (dashed line) at waypoint #427 on transect A18, located about 250 m offshore of the shoreline.

(within ~ 1 cm of penetration depth). The associated penetration velocity decreases from an initial impact velocity of almost 5 m/s in a pattern typically observed for sandy sediments and this type of devices [12, 13, 19].

Figure 7 shows the same information as Figure 6 from WPT #427 also located along transect A18, but only about 250 m from the shoreline. The initial impact velocity is also about 5 m/s, allowing a direct comparison of the deceleration profiles. Here, clear differences to the profile from WPT #418 can be identified. A soft top layer of about 6 cm in thickness can be distinguished before the sediment resistance, and thus deceleration, increases rapidly to a maximum deceleration of 70 g at a penetration depth of only 9 cm. This means that the seabed surface is overall significantly harder at WPT #427 over WPT #418. However, this hard seabed surface is covered with a thin (~6 cm) veneer of loose sand. Considering local sediment sources, the presence of a soft and muddy top layer can be excluded. Such loose seafloor sediment top layers in energetic nearshore environments have been associated with local sediment remobilization processes that are driven by currents and/or waves [12].

The deceleration-depth profiles of all deployment locations along transect A18 are displayed in Figure 8. All deployments feature a loose sediment top layer ranging from ~2-6 cm in thickness. However, the maximum deceleration and associated penetration depth suggest significant differences in surficial seabed hardness. The same information for transect L19 is provided in Figure 9, showing significantly more homogeneity along the transect. However, the profiles between A18 and L19 are fairly consistent among the harder locations. It appears that the looser seafloor conditions such as displayed in

Figure 6 and more present further offshore at Point Carrew cannot be detected along transect L19. As the presence of muddy to silty sediments that may be softer is unlikely at these locations, it can be hypothesized that the observed differences can be related to differences in relative density of the sandy sediment.

Equation 1 [20] was applied to all maximum decelerations that were measured within the uppermost 15 cm of the seabed surface. The resulting estimates of relative density are shown in Figure 10. Transects A18 and D18, both located in front of Point Carrew featured a wide range of maximum decelerations ranging from 16-79 g,

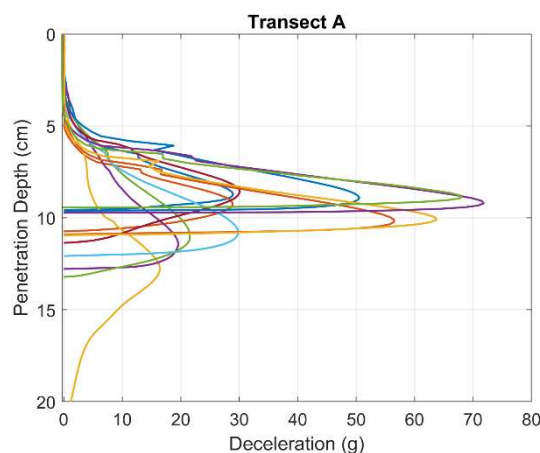


Figure 8. Penetration depth versus measured deceleration for all deployment locations along transect A18. The yellow profile of maximum penetration depth shows the penetrometer falling over after reaching a maximum deceleration, and therefore, data at penetration depths in excess of 13 cm should be ignored.

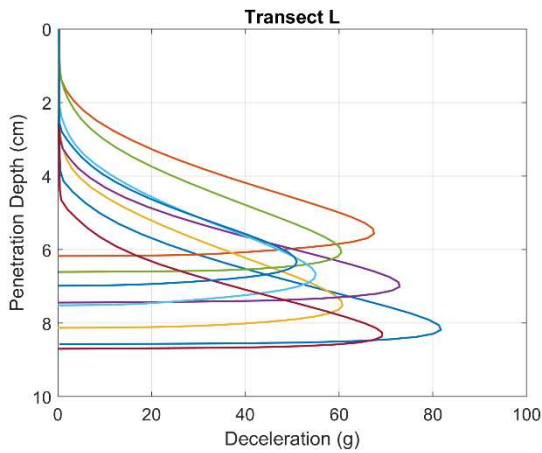


Figure 9. Penetration depth versus measured deceleration for all deployment locations along transect L19.

leading to estimates of relative density ranging from loose sands of $D_r < 20\%$ to very dense sand with $D_r > 90\%$. The variability is more limited along the Ocean Cape transects with maximum decelerations of 65-95 g and D_r ranging from 65-95 %. It can be observed in all transects that higher maximum decelerations and higher estimates of relative density were generally found closer to the shoreline, with some exceptions that may be related to localized processes (e.g., small-scale bedforms, recent event that stirred up sediment like boat engines). Therefore, the estimates of relative density were plotted against local water depth (Fig. 11).

A clear trend of increasing relative densities with decreasing water depths can be observed for water depths from 7-25 m along transects A18, L19 and L19. Transect D18 is excluded from this analysis due to erroneous water depth values resulting from a sensor issue. Measurements at water depths of ~5 m did not follow the same trend. For such shallow water depths, the relative density would be projected towards 100%. However, estimates based on the measurements suggested 75-92% (Fig. 11).

Impact velocities varied somewhat from about 4.1 m/s to 5.8 m/s for all deployments (similar to impact velocities measured by [20] when developing Eq. 1). They did not exhibit noticeable differences between the sites, however, with water depth. For example, most deployments at water depths < 13 m achieved impact velocities of 5-

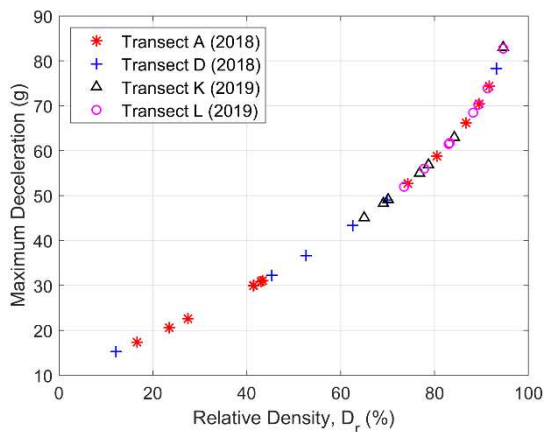


Figure 10. Estimated relative density from maximum deceleration values using equation 1 for all four transects.

5.8 m/s, while most deployments at water depths > 13 m yielded impact velocities of 4.1-5 m/s. This can be explained with increasing rope drag with deeper water depths [21]. While the variation in impact velocity was limited, somewhat of an exacerbating effect on the observed trends in relative density cannot be excluded without further investigations of rate effects. This will be explored in the future, investigating the application of strain rate corrections as well as impact velocity dependent parameters such as the firmness factor [13, 22]. Based on the limited range of variations in impact velocity, observations such as shown in Figures 6 and 7, and the more significant differences at shallow water depths, it can be assumed that the trends may be exacerbated but not qualitatively changed from effects of impact velocity.

A densification of sandy sediment by ocean wave forcing has been proposed before [23, 24]. Here, the results suggest that the relative density of sandy sediments increases with a decrease in water depth. A shallower water depth leads to a stronger interaction of wave energy with the seabed. A stronger interaction between the seabed and the waves would also suggest more sediment remobilization and a higher risk of sand liquefaction. Both mechanisms could contribute to the densification of sand. Overall lower values of relative density were found at Point Carrew where wave energy is lower. However, the large sand spit at Point Carrew also experienced a large sediment erosion event years ago, and it can be hypothesized that some material may be deposited offshore of the spit. The hypothesized sediment deposition combined with the low wave energy may explain the observations.

Wave conditions were of low energy when the surveys were conducted. However, waves were still breaking close to the shore. This means active sediment remobilization processes with current stirring of surface sediments may have been restricted to shallow water depths at the time of the survey. This would explain why measurements at 5 m of water depth departed from the general trend between water depth and relative density. Another reason may be more recent active sediment exchange with the beach at such shallow water depths. While these represent valid hypotheses, the current data set is not sufficient to confirm this.

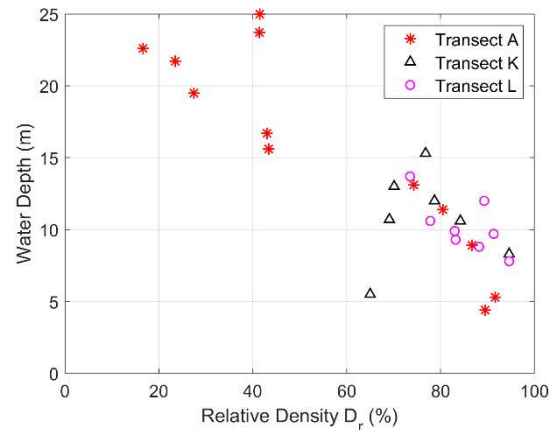


Figure 11. Estimated relative density versus water depth at the time of measurement. Please note that transect D18 was removed from this assessment due to erroneous water depth measurements.

This article presents a first application of the proposed method to estimate relative density from portable free fall penetrometer deployments for the investigation of spatial variations within the nearshore zone of a geomorphologically active peninsula. The retrieval of undisturbed sediment cores is currently highly challenging as sediment sampling and coring options that offer safe and easy deployment options (e.g., grab samplers, small gravity driven corers) struggle to recover samples from dense sandy seabeds. Additionally, options optimized for sandy sediments (e.g., vibrocorers) can be difficult to manage safely in energetic environments and also bear the potential to densify the sand while penetrating the soil through vibration. This issue represents the motivation for the development of the method [13, 20], but also represents the main challenge of the same method regarding validation of the results. This leaves at this point only a more holistic argumentation to evaluate the results. The overall range of estimated relative densities is wide but feasible, and processes possibly providing an explanation for the wide range of relative densities can be identified, namely, somewhat of exacerbation by rate effects, sand densification by wave action [23,24] and stirring and loose re-deposition of sand associated with sediment remobilization processes [12, 25]. Sediment sampling has confirmed that the sediment composition in the tested areas is sandy and that softer locations are unlikely resulting from the presence of fine-grained sediments. Similar variations in sediment strength along cross-shore transects in energetic nearshore zones have been observed in other locations as well as close to the test area before [12, 19]. However, in those studies no spatial comparison of estimates of relative densities were provided, yet, but the investigators pointed at the likelihood of variations in sediment strength resulting from strong spatial and temporal variations in relative density from hydrodynamically driven sediment reorganization and remobilization processes.

Estimating relative densities of surficial sands in nearshore environments has the potential of providing important information to improve the assessment of sediment erodibility and mobility (being dependent on particle packing [26]), as well as to enhance risk assessment for coastal structures from scour as well as sediment relocation processes [27] and for naval applications [28, 29]. The approach tested here is applicable in energetic nearshore conditions. Limitations in environmental conditions are mostly related to the vessel or platform safety rather than to the penetrometer. The method to estimate relative density yielded feasible values that can be explained with environmental conditions and governing factors, but further investigations are needed to increase confidence in the quantitative results and propose possible improvement regarding rate effects. The development of a novel sediment sampler unit for extraction of high quality sediment surface samples while penetrometer testing by Bilici and Stark (2019) [30] is currently being finalized for sampling of cohesionless and loose sands, and may provide new opportunities for validation.

5. Conclusions

A new approach to derive an estimate of relative density of sandy seabed surface sediments [13, 20] was preliminarily tested with regards to the investigation of spatial variations in relative density along four cross-shore transects off the Phipps Peninsula, Yakutat, Alaska. In this approach, a portable free fall penetrometer was used to measure differences in local sediment strength and estimate relative density of surficial seafloor sands. The data shown represents a part of a larger research study that aims for the investigation of the relationship between geotechnical parameters and coastal geomorphodynamics under energetic hydrodynamic conditions. The results showed significant variations in local surficial sediment strength, and thus, local relative density of the sandy seabed surface. Estimated relative densities reached from about 20% to 95%, representing a wide range but feasible results. A trend of increasing relative density with decreasing water depth (i.e., approaching the shoreline) was observed from 8-25 m of water depth. Measurements at water depths shallower than 6 m deviated from this trend. The observed variations and trends in estimated relative density can likely be explained by sand densification by ocean wave action and local sediment remobilization processes, but may be exacerbated by effects of variations in impact velocity. Results as presented here have the potential to contribute to the understanding of coastal geomorphodynamics, as well as to assist with naval applications and coastal engineering actions. Future steps will include a more detailed analysis of the full data set, the investigation of effects of impact velocity, the application of the same approach to other study areas and times, and improved validation of the results using a novel seafloor sediment sampler and physical simulations.

Acknowledgement

The project presented in this article is supported by the National Science Foundation (NSF) through grant CMMI-1751463. The authors would also like to thank the Yakutat 2018 and 2019 field teams, as well as the City and Borough of Yakutat, namely the late Rhonda Coston, Jon Erickson and Irving Grass.

References

- [1] Davis, R. A. "Beach and nearshore zone." In: Coastal sedimentary environments. Springer, New York, NY, pp. 379-444, 1985. https://doi.org/10.1007/978-1-4612-5078-4_6
- [2] Dietz, Robert S. "Wave-base, marine profile of equilibrium, and wave-built terraces: a critical appraisal." Geological Society of America Bulletin, 74(8), pp. 971-990, 1963.
- [3] Elgar, S., Gallagher, E. L., & Guza, R. T. "Nearshore sandbar migration." Journal of Geophysical Research: Oceans, 106(C6), pp. 11623-11627, 2001. <https://doi.org/10.1029/2000JC000389>
- [4] Ruessink, B. G., Van Enkevort, I. M. J., & Kuriyama, Y. "Non-linear principal component analysis of nearshore bathymetry." Marine Geology, 203(1-2), pp. 185-197, 2004. [https://doi.org/10.1016/S0025-3227\(03\)00334-7](https://doi.org/10.1016/S0025-3227(03)00334-7).
- [5] Schupp, C. A., McNinch, J. E., & List, J. H. "Nearshore shore-oblique bars, gravel outcrops, and their correlation to shoreline change." Marine Geology, 233(1-4), pp. 63-79, 2006. <https://doi.org/10.1016/j.margeo.2006.08.007>

- [6] Ruggiero, P., Walstra, D. J. R., Gelfenbaum, G., & Van Ormondt, M. "Seasonal-scale nearshore morphological evolution: Field observations and numerical modeling." *Coastal Engineering*, 56(11-12), pp. 1153-1172, 2009. <https://doi.org/10.1016/j.coastaleng.2009.08.003>
- [7] Ruessink, B. G., & Kuriyama, Y. "Numerical predictability experiments of cross-shore sandbar migration." *Geophysical Research Letters*, 35(1), 2008. <https://doi.org/10.1029/2007GL032530>
- [8] Plant, N. G., Holland, K. T., Puleo, J. A., & Gallagher, E. L. "Prediction skill of nearshore profile evolution models." *Journal of Geophysical Research: Oceans*, 109(C1), 2004. <https://doi.org/10.1029/2003JC001995>
- [9] White, T. E. "Nearshore Sand Transport." California Univ San Diego La Jolla, USA, 1987.
- [10] Douglass, S. L. "Estimating landward migration of nearshore constructed sand mounds." *Journal of waterway, port, coastal, and ocean engineering*, 121(5), pp. 247-250, 1995. [https://doi.org/10.1061/\(ASCE\)0733-950X\(1995\)121:5\(247\)](https://doi.org/10.1061/(ASCE)0733-950X(1995)121:5(247))
- [11] Caballeria, M., Coco, G., Falqués, A., & Huntley, D. A. "Self-organization mechanisms for the formation of nearshore crescentic and transverse sand bars." *Journal of Fluid Mechanics*, 465, pp. 379-410, 2002. <https://doi.org/10.1017/S002211200200112X>
- [12] Albatal, A., Wadman, H., Stark, N., Bilici, C., & McNinch, J. "Investigation of spatial and short-term temporal nearshore sandy sediment strength using a portable free fall penetrometer." *Coastal Engineering*, 143, pp. 21-37, 2019. <https://doi.org/10.1016/j.coastaleng.2018.10.013>
- [13] Albatal, A., Stark, N., & Castellanos, B. "Estimating in-situ relative density and friction angle of nearshore sand from portable free fall penetrometer tests." *Canadian Geotechnical Journal*, 57(1), pp. 17-31, 2020. <https://doi.org/10.1139/cgj-2018-0267>
- [14] Tschetter, T., Kasper, J.L., & Duvoy, P.X. "Yakutat bay wave resource assessment." Alaska Center for Energy and Power, University of Alaska, Fairbanks.
- [15] Ruby, C.H. "Coastal morphology, sedimentation and oil spill vulnerability, northern Gulf of Alaska." Tech. Report No. 15-CRD, University of South Carolina, 1977.
- [16] Wright, F. F. "Marine geology of Yakutat Bay, Alaska." US Geological Survey Professional Paper, 800, pp. 9-15, 1972.
- [17] Masselink, G., & Short, A. D. "The effect of tide range on beach morphodynamics and morphology: a conceptual beach model." *Journal of coastal research*, pp. 785-800, 1993.
- [18] Oblinger, A., & Anthony, E. J. "Surface moisture variations on a multibarred macrotidal beach: implications for aeolian sand transport." *Journal of Coastal Research*, pp. 1194-1199, 2008.
- [19] Albatal, A., & Stark, N. "In Situ Geotechnical Early Site Assessment of a Proposed Wave Energy Converter Site in Yakutat, Alaska, Using a Portable Free-Fall Penetrometer." In *Geo-Chicago 2016*, pp. 429-438, 2016.
- [20] Albatal, A. "Advancement of using portable free fall penetrometers for geotechnical site characterization of energetic sandy nearshore areas." Ph.D. Dissertation submitted to the Department of Civil and Environmental Engineering, Virginia Tech, Blacksburg, VA, USA, 2018
- [21] Stark, N., & Ziotopoulou, K. "Undrained shear strength of offshore sediments from portable free fall penetrometers: theory, field observations and numerical simulations." In: *Offshore Site Investigation Geotechnics 8th International Conference Proceeding*, 391(399), pp. 391-399, 2017. <https://doi.org/10.3723/OSIG17.391>
- [22] Mulukutla, G. K., Huff, L. C., Melton, J. S., Baldwin, K. C., & Mayer, L. A. "Sediment identification using free fall penetrometer acceleration-time histories." *Marine Geophysical Research*, 32(3), pp. 397-411, 2011. <https://doi.org/10.1007/s11001-011-9124-2>
- [23] Clukey, E. C., Jackson, C. R., Vermersch, J. A., Koch, S. P., & Lamb, W. C. "Natural densification by wave action of sand surrounding a buried offshore pipeline." In: *Offshore Technology Conference. Offshore Technology Conference, Houston, Texas, May 1-4 1989, OTC-6151-MS*, 1989. <https://doi.org/10.4043/6151-MS>
- [24] Zen, K., & Yamazaki, H. "Mechanism of wave-induced liquefaction and densification in seabed." *Soils and foundations*, 30(4), pp. 90-104, 1990. https://doi.org/10.3208/sandf1972.30.4_90
- [25] Stark, N., & Kopf, A. "Detection and quantification of sediment remobilization processes using a dynamic penetrometer." In *MTS/IEEE OCEANS'11, Kona, Hawaii, USA, Sept 19-22 2011*, 2011. 10.23919/OCEANS.2011.6106914
- [26] Kirchner, J. W., Dietrich, W. E., Iseya, F., & Ikeda, H. "The variability of critical shear stress, friction angle, and grain protrusion in water-worked sediments." *Sedimentology*, 37(4), pp. 647-672, 1990. <https://doi.org/10.1111/j.1365-3091.1990.tb00627.x>
- [27] Abanades, J., Greaves, D., & Iglesias, G. Wave farm impact on the beach profile: A case study. *Coastal Engineering*, 86, pp. 36-44, 2014. <https://doi.org/10.1016/j.coastaleng.2014.01.008>
- [28] Richardson, M., Valent, P., Briggs, K., Bradley, J., & Griffin, S. "NRL mine burial experiments." Naval Research Lab Stennis Space Center Ms Marine Geosciences Div., 2001. <https://apps.dtic.mil/dtic/tr/fulltext/u2/a403441.pdf>
- [29] Wiendieck, K. W. "A Preliminary Study of Seafloor Trafficability and Its Prediction (No. Aewes-Tr-M-70-8)." Army Engineer Waterways Experiment Station Vicksburg Miss., 1970. <https://apps.dtic.mil/docs/citations/AD0710965>
- [30] Bilici, C., & Stark, N. "Performance of a novel sediment sampler as an add-on unit for portable free-fall penetrometers: Combining in situ geotechnical testing with sediment sampling." *Limnology and Oceanography: Methods*, 17(2), pp. 163-176, 2019. <https://doi.org/10.1002/lom3.10308>
- [31] Google Earth. Image Landsat/Copernicus, Image @2019 CNES/Airbus, Image @Maxar Technologies. Image date: June 25 2019. Last accessed on Google Earth Pro: September 24, 2019.